Available online at www.sciencedirect.com

ScienceDirect

IFAC PapersOnline CONFERENCE PAPER ARCHIVE

IFAC PapersOnLine 55-37 (2022) 376–381

Integrated inverted pendulum and whole-body control design for bipedal robot with foot slip

Marko Mihalec * **Feng Han** * **Jingang Yi** *

* *Department of Mechanical and Aerospace Engineering Rutgers University, Piscataway, NJ 08854 USA (email: {marko.mihalec, fh233, jgyi}@rutgers.edu)*

Abstract: Low-friction ground surfaces present a particular challenge for control of bipedal walking robots. The onset of foot slip changes the robot dynamics and the commonly designed walking controllers assuming non-slip conditions cannot maintain balance and prevent the walker from falling. We present a two-level robot controller for bipedal walker under foot slip. The high-level control is built on a two-mass linear inverted pendulum (TMLIP) model to generate the appropriate step location such that the robot walker maintains dynamic balance through multiple planned steps. The specified stepping tasks are fed to the low-level control that is based on a whole-body operational space (WBOS) framework. The WBOS controller uses the dynamic model of the multi-link bipedal walker and generates joint torques to maintain balance and follow the given stepping task in the presence of foot slip. Performance of the integrated TMLIP-WBOS control algorithm is demonstrated through extensive simulation studies of a 5-link robotic walker.

Keywords: Bipedal walker, slip, balance control, gait stability, motion control

1. INTRODUCTION

Legged locomotion allows traversing rugged and unstructured terrain, such as stepping over obstacles, or up and down stairs. However, bipedal walking comes with a different set of challenges such as a dependence on particular frictional conditions between the walker's feet and the ground. The majority of existing research work that are relevant to low-friction foot contact aims to avoid slip a priori. For example, Khadiv et al. (2017) used an optimization approach to identify a feasible gait pattern under which the biped requires the lowest coefficient of friction, while Ferreira et al. (2020) proposed a bipedal gait controller that used wearable friction sensors to adjust gait parameters to avoid foot slipping. The main goal of this work is to address the gait control challenge of bipedal walking on low-friction surfaces in presence of foot slip.

Explicit studies on slip dynamics remain comparatively scarce. Chen and Goodwine (2021) presented dynamics of compass gait under slip, while Ma et al. (2019) experimentally demonstrated balancing a planar walking robot with expected slip at the beginning of each step with. Research works that explicitly examine the slipping dynamics are predominately focused on human locomotion. To that extent, Chen et al. (2015) presented a model for describing human walking with foot slip, while Trkov et al. (2019, 2020) presented control and detection of human walking under foot-slip conditions. Similarly, the recent work in Mihalec et al. (2022) considered a simplified dynamic model and demonstrated the agreement of the model with human slip and fall gait.

To design a model-based recovery control under foot slip, we need to deal with gait planning and trajectory following. Due to the high-dimensional bipedal robots and the complexity of the walking task, gait controller is usually constructed hierarchically. In Reher and Ames (2021), a top control layer deals with high-level motion planning with trajectory generation, a mid-level control layer includes stability control of reduced-order models, and a low-level control layer provides joint torques of the full-body dynamics. For biped gait generation, the commonly used model is the inverted pendulum model (Kajita et al., 2001). By constraining the center of mass (CoM) to a constant height, a linear inverted pendulum (LIP) model is obtained and provides simple, closed-form trajectory profiles. However, due the LIP model's assumptions such as all the mass being concentrated at a single point, a simple LIP model is not suitable for gaits under foot slip. A two-mass LIP (TMLIP) model was introduced to overcome such shortcomings (Mihalec et al., 2020). The TMLIP model retains the linear nature of the dynamics and simultaneously allows for modeling of arbitrary ground reaction forces and for gaits with foot slip. The linear dynamics of a reduced-order model yields a closed-form solution which can be used to introduce the concept of motion manifolds (Zhao et al., 2017). In Mihalec et al. (2020, 2021), motion manifolds were used to capture the slip dynamics and unify the modeling framework under normal walking and slip cases.

To implement the LIP model-based control strategy, joint torques are needed and therefore, we need to build a whole-body controller for multi-link bipedal robots. One such approach is the whole-body operational space (WBOS)

10.1016/j.ifacol.2022.11.212

that was proposed in Khatib (1987). The WBOS uses inverse dynamics to map a set of kinematic tasks to joint torques and it has been shown to successfully generate stable walking gaits (Luo et al., 2017, 2019). Recently, a modification of WBOS, called Frictional WBOS (FWBOS), was presented in Mihalec and Yi (2021). The FWBOS allows for modeling of non-stationary contact between the robot foot and the ground and thus enables the study of walking under foot-slip conditions. The FWBOS uses Coulomb frictional forces at the moving contact point between the robot and the ground to replace the stationary foot assumptions.

This paper presents an integrated bipedal walking controller with explicit consideration of foot slip. The control algorithm uses the TMLIP model to predict stepping locations and integrates the planning strategy with the FWBOS-based torque controller. The distinct advantage of using the TMLIP model and the FWBOS is that it preserves a unified gait generation and low-level joint torque implementation for both slip and non-slip cases. The proposed controller is implemented on a 5-link robot in simulation environment and the results demonstrate its performance. The main contribution of this work lies in providing a novel, comprehensive slip controller, which for the first time presents a unified reduced-order and full-body controller. Both the reduced-order and full-body models are specifically adapted to foot-slip and explicitly consider the changing dynamics under slipping conditions. Furthermore, an acceleration task is specified for the FWBOS controller for the first time and we show that it yields stable dynamics.

The remainder of this paper is organized as follows. Section 2 introduces the integrated TMLIP and FWBOS models. The proposed control algorithms are given in Section 3. Section 4 presents the simulation results before we summarize the concluding remarks in Section 5.

2. DYNAMIC MODELS OF THE BIPED WALKER

In this section, we describe the reduced-order TMLIP model and a full-order 5-link model for robotic walker. Figure 1(a) illustrates the schematic of the TMLIP model and Fig. 1(b) for the full-body 5-link model for a biped walker.

2.1 Reduced-order LIP model

We use the two-mass LIP model introduced in Mihalec et al. (2020). For reader's convenience, the key features of the model are summarized here. As shown in Fig. 1(a), the model consists of two point masses, with the larger mass, denoted as m_1, at the horizontal location x_c representing the CoM and being equivalent to the widely used LIP model (Kajita et al., 2001). The smaller point mass, denoted as m_2, represents the mass contribution of the lower standing leg and is located at x_f, the contact point between the robot and the ground.

During normal (non-slip) walking, that is, $\dot{x}_f = 0$, the TMLIP model is identical to the single-mass LIP model; however, during foot-slip of the standing leg $\dot{x}_f \neq 0$, the TMLIP model retains finite angular accelerations and is able to explicitly model the slipping dynamics. We define

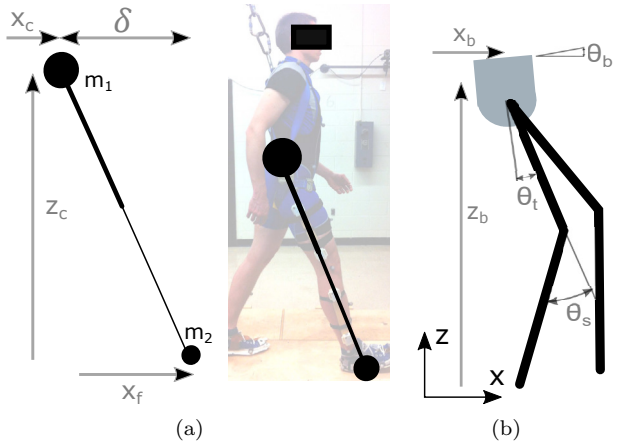

Fig. 1. (a) Schematic of the two-mass LIP model. (b) Schematic of a 5-link full-body model.

the horizontal distance between the two masses as $\delta = x_c - x_f$ such that $\delta \geq 0$ when m_1 is anterior or in front of m_2 along the direction of walking. The dynamic equation for the TMLIP model is written as (Mihalec et al., 2021)

$$\ddot{\delta} = \omega_m^2(\delta + A), \tag{1}$$

where constants $A = 0$ and $\omega_m^2 = \omega^2$ are used for the non-slip case and $A = \mu z_c$ and $\omega_m^2 = \frac{r_m}{r_m - 1}\omega^2$ with $r_m = \frac{m_1 + m_2}{m_1}$, when the standing foot slips with respect to the ground. μ denotes the friction coefficient and $\omega = \sqrt{g/z_c}$ is the natural frequency of the LIP model, where g is gravitational acceleration and z_c is the height of m_1 above the ground.

By analytically solving (1), motion manifolds are obtained as

$$\frac{(\delta + A)^2}{(\delta_0 + A)^2 - \dot{\delta}_0^2/\omega_m^2} - \frac{\dot{\delta}^2/\omega_m^2}{(\delta_0 + A)^2 - \dot{\delta}_0^2/\omega_m^2} = 1, \tag{2}$$

where $(\delta_0, \dot{\delta}_0)$ is the initial condition defining a specific manifold. In the absence of external perturbations, the dynamics of the TMLIP model is confined to a single manifold and therefore, the motion of the model is predicted both for slip and non-slip cases, with manifolds (2) in the δ-$\dot{\delta}$ state space plane. For more details about solution manifolds for TMLIP, the reader is referred to Mihalec et al. (2022).

2.2 Full-order multi-link model

The full-order model is a planar 5-link structure that consists of a passive floating base and two actuated parallel chains serving as the thighs and the shanks of robot's legs; see Fig. 1(b). The state of the model is defined by $\boldsymbol{q} = [x_b \;\; z_b \;\; \theta_b \;\; \theta_t^c \;\; \theta_s^c \;\; \theta_t^f \;\; \theta_s^f]^T \in \mathbb{R}^7$, where the first three components x_b, z_b, θ_b define the position and orientation of the floating base in the sagittal plane, θ_t and θ_s are the relative thigh and shank angles, respectively. Superscripts c and f denote the contact and the free/swing leg, respectively. The parameters for the 5-link model were selected to roughly match a typical adult human as in Winter (2009). Table 1 lists the definitions and values of the model parameters.

The motion equation of the full-order dynamics model is written as

$$\boldsymbol{A}\ddot{\boldsymbol{q}} + \boldsymbol{N}_s^T(\boldsymbol{b}+\boldsymbol{g}) + \boldsymbol{J}_s^T\boldsymbol{\Lambda}_s\dot{\boldsymbol{J}}_s\dot{q} = (\boldsymbol{S}\boldsymbol{N}_s)^T\boldsymbol{\Gamma}, \quad (3)$$

where $\boldsymbol{A}$ is the inertia matrix, $\boldsymbol{b}$ and $\boldsymbol{g}$ are the vectors of Coriolis and centrifugal forces and gravitational forces, respectively. $\boldsymbol{\Lambda}_s$ denotes the mass inertia matrix associated with the contact point, and $\boldsymbol{J}_s$ and $\boldsymbol{N}_s$ represent the contact Jacobian and its null-space, respectively. $\boldsymbol{\Gamma}$ is the vector of joint torques while $\boldsymbol{S}$ is the selection matrix defining the rows of $\boldsymbol{q}$ that correspond to actuated joints. The reader can refer to Mihalec and Yi (2021) for details.

Table 1. Parameters of the 5-link model

Parameter	Symbol	Value
Thigh length	L_t	428.8 mm
Shank length	L_s	498.7 mm
Thigh CoM length	$L_{t,c}$	214.4 mm
Shank CoM length	$L_{s,c}$	249.4 mm
Mass of the base	m_b	47.46 kg
Mass of the thigh	m_t	7.00 kg
Mass of the shank	m_s	4.27 kg
Thigh angular inertia	I_t	0.134 kg m^2
Shank angular inertia	I_s	0.097 kg m^2

To use both the reduced- and the full-order model as a part of the control algorithm, we discuss the integration of these two models. For a robot with mass parameters such as those specified in Table 1, the ratio of the masses is estimated to be $r_m = (m_b + m_s)/m_s \gg 1$. The configuration of the TMLIP model is derived such that the mass m_1 is positioned in the CoM as

$$z_c = \frac{1}{M}\left[z_b m_b + (z_t^c + z_t^f)m_t + (z_s^c + z_s^f)m_s\right],$$
$$x_c = \frac{1}{M}\left[x_b m_b + (x_t^c + x_t^f)m_t + (x_s^c + x_s^f)m_s\right].$$

Here, $M = m_b + 2m_t + 2m_s$ is the total mass of the model while the locations for the CoM for each individual link are given in the vertical direction as

$$z_t^i = z_b - L_b\cos\theta_b - L_{t,c}\cos(\theta_b + \theta_t^i),$$
$$z_s^i = z_b - L_b\cos\theta_b - L_t\cos(\theta_b + \theta_t^i) - L_{s,c}\cos(\theta_b + \theta_t^i + \theta_s^i)$$

and in the horizontal direction as

$$x_t^i = x_b + L_b\sin\theta_b + L_{t,c}\sin(\theta_b + \theta_t^i),$$
$$x_s^i = x_b + L_b\sin\theta_b + L_t\sin(\theta_b + \theta_t^i) + L_{s,c}\sin(\theta_b + \theta_t^i + \theta_s^i)$$

for $i \in c, f$ and the variables in the above equations are defined in Table 1. The point mass m_2 is positioned at the point where the 5-link model contacts the ground:

$$x_f = x_b + L_b\sin\theta_b + L_t\sin(\theta_b + \theta_t^c) + L_s\sin(\theta_b + \theta_t^c + \theta_s^c).$$

3. WALKING WITH SLIP CONTROLLER

This section presents the control algorithm for safe walking on slippery surfaces, both in the absence and presence of foot slip. Fig. 2 illustrates the main structure of the algorithm design. While the relationship between the full- and the reduced-order models was presented in the previous section and we here specify the remaining three components: step planner, task specification, and whole-body control.

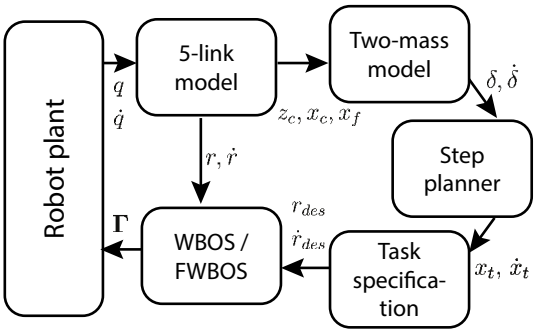

Fig. 2. Control algorithm for walking in presence and absence of foot slip

Step planner uses the known TMLIP model to obtain an adequate stepping location. Task specification uses the desired stepping location and the current position to determine a gradual trajectory between the current pose and the desired configuration at the end of the step. Finally, WBOS and FWBOS are used to transform the desired trajectories into joint torques. The control algorithm uses exclusively algebraic expressions in design, assuring feasibility for real-time applications. Note that the sequence of the controller remains the same regardless of the presence or absence of foot slip. With the onset of slip, the only changes are the A and ω_m values of the two-mass model and the use of FWBOS instead of WBOS.

3.1 Step location

The step location is based on the stability of the TMLIP model; however, two parameters need to be specified by the user: the stepping frequency f and the desired forward progression velocity $\dot{\delta}_i$. Since the velocity varies within a single step, $\dot{\delta}_i$ is specified in terms of infimum velocity, that is, the lowest velocity occurring during periodic gait and is achieved at $\delta = -A$. For the case without foot slip, infimum velocity is equivalent to apex velocity Zhao et al. (2017). For forward progression, positive $\dot{\delta}_i$ is selected, while $\dot{\delta}_i = 0$ commands the robot to come to a stop.

Next, we define δ_m, that is, the desired configuration of the robot at the beginning of the step. Using the motion manifolds (2), δ_m is obtained by setting $(\delta_0, \dot{\delta}_0) = (-A, \dot{\delta}_i)$, resulting in

$$\delta_m = -A + \frac{1}{\omega_m}\sqrt{\dot{\delta}_m^2 - \dot{\delta}_i^2}. \quad (4)$$

$\dot{\delta}_m$ is the forward progression after the step is taken, which is, due to uncertainties stemming from impact dynamics, approximated with the current forward progression $\dot{\delta}_m = \dot{\delta}$. With the known configuration δ_m, the desired touchdown location x_t is given by

$$x_t = x_c(t_t) + \delta_m, \quad (5)$$

where $x_c(t_t)$ denotes the predicted CoM location at the time of heel strike and is estimated as $x_c(t_t) = x_c(t) + \dot{x}_b(1/f - t)$. We now use the desired touchdown location x_t to specify the swing foot trajectory.

3.2 Task specification

The vector for desired tracking references is specified as

$$\boldsymbol{r}_{des} = [z_{CoM}\ \theta_b\ x_f(t)\ z_f(t)]^T, \tag{6}$$

where z_{CoM} is a constant height of the CoM and $\theta_b = 0$ is the angle of the torso. Angle θ_b specifies the torso to constantly maintain in vertical orientation. $x_f(t)$ is the horizontal location of the swing foot specified as a smooth 5^{th}-order polynomial trajectory between the takeoff and touchdown location of the swing foot, that is,

$$x_f(t) = a_0 + a_1 t + a_2 t^2 + a_3 t^3 + a_4 t^4 + a_5 t^5. \tag{7}$$

The coefficients of the polynomial are selected using the current position x_0 and velocity $\dot{x}_0$ of the free foot at the current time $t = t_0$. The desired touch-down $t = t_t$ position x_t and velocity $\dot{x}_t$ are specified by the step planner such that $x_f(t_0) = x_0$, $\dot{x}_f(t_0) = \dot{x}_0$, $x_f(t_t) = x_t$, and $\dot{x}_f(t_t) = \dot{x}_t$. Finally, $\ddot{x}_f(t_t) = 0$ ensures accurate tracking close to the location of the heel-strike. In order to assure a smooth trajectory, the initial jerk is specified as $\dddot{x}_f(t_0) = 0$. By solving (7), the desired instantaneous acceleration is specified as

$$\ddot{x}_f(t_0) = -\frac{2}{3t_r^2}(5x_0 - 5x_f + 3t_r v_0 + 2t_r v_t),$$

where $t_r = t_t - t_0$ is the time remaining until the heel-strike. The values for t_r, $x_f(t)$, and $\ddot{x}_f(t_0)$ are recalculated at every time instance to take into account disturbances and uncertainties.

The vertical location of the swing foot $z_f(t)$ is specified by a sin wave. To ensure the free foot touches the ground despite possible tracking error, a decreasing quadratic term is added, such that the complete vertical trajectory follows the function

$$z_f(t) = \frac{z_0}{2} + \frac{z_0}{2}\sin(2\pi f t - \frac{\pi}{2}) - B(ft)^2, \tag{8}$$

where z_0 is the maximum desired height of the foot. B is a parameter of a negative quadratic term which ensures that the free foot contacts the ground at the end of the swing phase at $t = t_t$.

The desired velocity $\dot{\boldsymbol{r}}_{des}$ and acceleration $\ddot{\boldsymbol{r}}_{des}$ terms are obtained by taking the time derivative of the desired position vector $\boldsymbol{r}$ as

$$\dot{\boldsymbol{r}}_{des} = [0\ 0\ \dot{x}_f(t)\ \dot{z}_f(t)]^T, \ddot{\boldsymbol{r}}_{des} = [0\ 0\ \ddot{x}_f(t)\ \ddot{z}_f(t)]^T. \tag{9}$$

3.3 WBOS and frictional WBOS

To obtain appropriate joint torques to execute the desired motion, the FWBOS framework is used with Coulomb friction model. For completion this section presents derivations of both WBOS and FWBOS.

In the WBOS framework, the motion is accomplished by specifying a generalized force $\boldsymbol{F}_{t|s}$ in task space which consists of acceleration $\boldsymbol{u}_{t|s}$, centrifugal and Coriolis forces $\boldsymbol{c}_{t|s}$, and gravity force $\boldsymbol{p}_{t|s}$, all expressed in task space,

$$\boldsymbol{F}_{t|s} = \boldsymbol{\Lambda}_{t|s}\boldsymbol{u}_{t|s} + \boldsymbol{c}_{t|s} + \boldsymbol{p}_{t|s}. \tag{10}$$

The trajectory to be tracked is specified with its acceleration $\boldsymbol{u}_{t|s}$ and is multiplied by the task space kinetic energy matrix $\boldsymbol{\Lambda}_{t|s}$. The exact form for $\boldsymbol{u}_{t|s}$ will be specified later in this section. The generalized force $\boldsymbol{F}_{t|s}$ is projected to the joint torques $\boldsymbol{\Gamma}$ by

$$\boldsymbol{\Gamma} = \boldsymbol{J}^{*T}\boldsymbol{F}_{t|s}, \tag{11}$$

where $\boldsymbol{J}^*$ is the reduced task Jacobian matrix consistent with support constraints $\boldsymbol{J}^* = \boldsymbol{J}_{t|s}(\overline{\boldsymbol{SN}_c})$ and $\boldsymbol{J}_{t|s}$ is the task Jacobian. $\overline{\boldsymbol{SN}_c}$ represents the generalized inverse of $\boldsymbol{SN}_s$, where $\boldsymbol{N}_s$ is the null space of support constraints, $\boldsymbol{N}_s = \boldsymbol{I} - \bar{\boldsymbol{J}}_s\boldsymbol{J}_s$.

In the case of foot slip, FWBOS is used and a Coulomb friction model is considered at the contact between the biped foot and the ground. Consequently, the generalized force for task space under frictional contact $\boldsymbol{F}^F_{t|s}$ is specified as

$$\boldsymbol{F}^F_{t|s} = \boldsymbol{\Lambda}^T_{t|s}\boldsymbol{u}_{t|s} + \boldsymbol{c}^F_{t|s} + \boldsymbol{p}^F_{t|s}, \tag{12}$$

where $\boldsymbol{c}^F_{t|s}$ and $\boldsymbol{p}^F_{t|s}$ are the frictional equivalents for the centrifugal/Coriolis and gravity forces, respectively. The above equations are obtained similarly to the non-slip case; however, the null space of the support constraint $\boldsymbol{N}$ is obtained for the Coulomb contact as $\boldsymbol{N}^T_f = \boldsymbol{I} - \boldsymbol{J}^T_s\boldsymbol{M}\bar{\boldsymbol{J}}^T_{sz}$, where $\boldsymbol{M} = [\mp\mu,\ 1]^T$. $\boldsymbol{J}_{sz}$ represents the reduced contact Jacobian that is obtained as a subset of the full contact Jacobian by $\boldsymbol{J}_{sz} = [0\ \ 1]\boldsymbol{J}_s$, and thus only prevents kinematic movement in the vertical z direction.

The mapping between the generalized task forces and joint torques is achieved by

$$\boldsymbol{\Gamma}_f = \boldsymbol{J}^{*T}_f\boldsymbol{F}^F_{t|s}.$$

The frictional support null-space $\boldsymbol{N}_f$ is used such that $\boldsymbol{J}^*_f = \boldsymbol{J}_{t|s}(\overline{\boldsymbol{SN}_f})$. For a more detailed derivation of the frictional WBOS framework, the reader is referred to Mihalec and Yi (2021). Kinematic trajectory of the desired task is specified in task acceleration as

$$\boldsymbol{u}_{t|s} = \ddot{\boldsymbol{r}}_{des} + \boldsymbol{k_p}\boldsymbol{e} + \boldsymbol{k_d}\dot{\boldsymbol{e}}, \tag{13}$$

where tracking error $\boldsymbol{e} = \boldsymbol{r}_{des} - \boldsymbol{r}_{act}$, $\boldsymbol{k_p}$ and $\boldsymbol{k_d}$ are the diagonal matrices representing the proportional and derivative PD gains, respectively.

With the control design (13), the closed-loop stability is achieved as follows. Using the control input $\ddot{\boldsymbol{r}}_{act} = \boldsymbol{u}_{t|s}$ and by (13), we obtain

$$\ddot{\boldsymbol{e}} = \ddot{\boldsymbol{r}}_{des} - \boldsymbol{u}_{t|s} = \ddot{\boldsymbol{r}}_{des} - \ddot{\boldsymbol{r}}_{des} - \boldsymbol{k}_p\boldsymbol{e} - \boldsymbol{k}_d\dot{\boldsymbol{e}}.$$

Rearranging the above expression yields error dynamics as $\ddot{\boldsymbol{e}} + \boldsymbol{k}_d\dot{\boldsymbol{e}} + \boldsymbol{k}_p\boldsymbol{e} = \boldsymbol{0}$. The asymptotic stability is obtained since $\boldsymbol{k}_p$ and $\boldsymbol{k}_d$ are selected as diagonal matrices with positive elements.

4. SIMULATION RESULTS

This section presents the simulation results of both walking on a non-slippery surface as well as slip recovery on a low-friction surface. The proposed controller from the above section was implemented in simulation of a planar 5-link robot. The control algorithm was implemented in Matlab/Simulink environment and control loop was executed at the rate of 1 kHz. For the simulation experimental setup, the proportional and derivative gains were selected as $\boldsymbol{k_p} = \text{diag}(120, 60, 300, 300)$ [s^{-2}] and $\boldsymbol{k_d} = \text{diag}(5, 5, 20, 50)$ [s^{-1}], respectively, and other model parameters' values are listed in Table 1.

4.1 Periodic walking

The simulation begins with the robot being stationary. The robot is set in motion and commanded to walk for

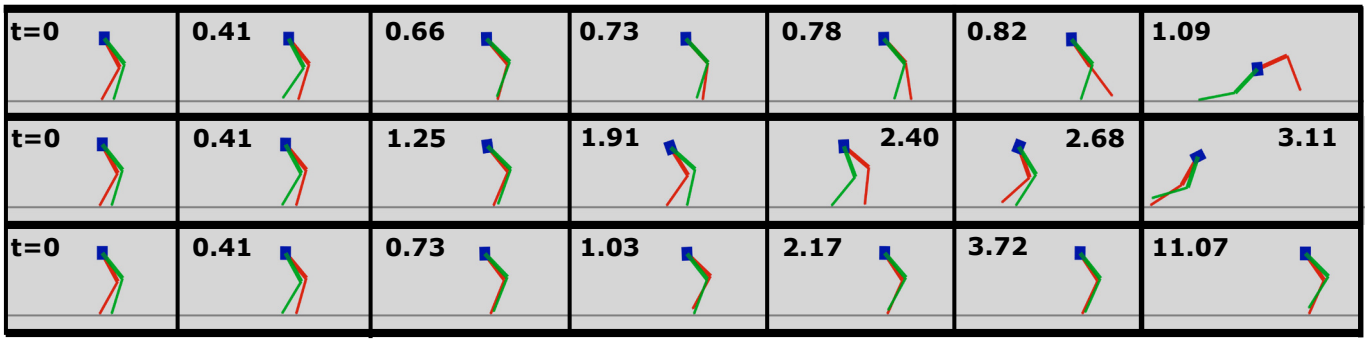

Fig. 3. Snapshot of recovery sequence. Top: not considering slip; middle: Using FWBOS but neglecting slip at step planning phase; bottom: using FWBOS and a TMLIP model with explicit consideration of foot slip.

30 steps in order to achieve periodic gait on high friction surface with $\mu = 0.5$. Figure 4 shows the gait of the WBOS-based controller during walking over high-friction ground and confirms that the walker was able to achieve periodic gait.

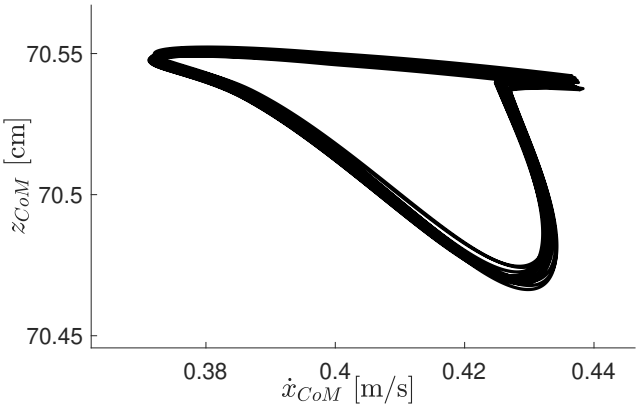

Fig. 4. The vertical height and forward progression of the CoM during periodic walking over high-friction ground.

The horizontal dynamics of the 5-link model is not controlled directly. It conforms to the natural dynamics within a single step and is only controlled as a series of step locations based on the TMLIP model. In order for the WBOS integration, the models must share similar horizontal dynamics. Figure 5 shows a comparison between the natural dynamics of the simulated 5-link robot and the theoretical dynamics of the TMLIP model. It can be seen that for periodic walking over high friction ground, the integrated models are in good agreement and these results confirm the integration of the models in Section 2.

4.2 Slip recovery

To demonstrate the advantages of the proposed control design for bipedal gait in the presence of foot slip, we present an evolution of slip recovery on a low-friction surface. To initiate the simulation, the walker was set in motion on a high friction surface ($\mu = 0.5$) where no slip is present. The biped was allowed to walk for 30 steps in order to establish periodic gait. After 30 steps, at time $t = 0$, the contact condition was modified and foot-floor friction was reduced to $\mu = 0.075$. After the reduction of

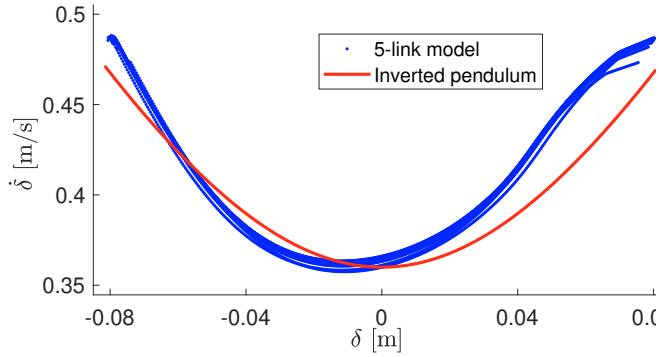

Fig. 5. Comparison of the results between the simulated dynamics of the 5-link model and theoretical dynamics of the TMLIP model.

the friction coefficient, the biped was commanded to stop by reducing the desired forward progression velocity to $\dot{\delta}_i = 0$.

Figure 3 shows the snapshots of the progression using three different controllers. First, a benchmark WBOS-based controller without any consideration of foot slip is shown in the top row. Under such a controller, the velocity of the slipping foot was divergent and the supporting foot accelerated forward making the robot fall within $t = 1.1$ s after the reduction of the friction coefficient. Next, the simulation was repeated with the FWBOS-based design while the step planner still assumed no slip. The FWBOS was able to limit the acceleration of the slipping foot and the walker was able to stop the forward progression. However, due to lack of effective step planner, the walker started moving backwards, before ultimately loosing balance due to slip and falling at $t = 3$ s. Finally, the control algorithm proposed in this paper was implemented with both the FWBOS-based whole-body controller and the TMLIP model-based step planner that explicitly considered foot slip; see the bottom row in Fig. 3. The proposed controller was able to maintain balance and remained stable despite the reduced friction. In order to maintain balance around non-stable equilibrium, the robot kept stable with small stepping corrections and rejecting disturbances.

Figure 6 further shows the horizontal velocity of the walker before and after reduction of the friction coefficient. It can be seen that only the proposed controller with consideration of slip at both high- and low-level was able

to reduce the forward progression and maintained balance near the stationary position. In comparison with other controllers, the results confirmed that not using FWBOS in the case of foot slip led to immediate fall, while using FWBOS with non-effective step planning, the robot might maintain balance for a short period but the controller was not able to adequately maintain horizontal progression.

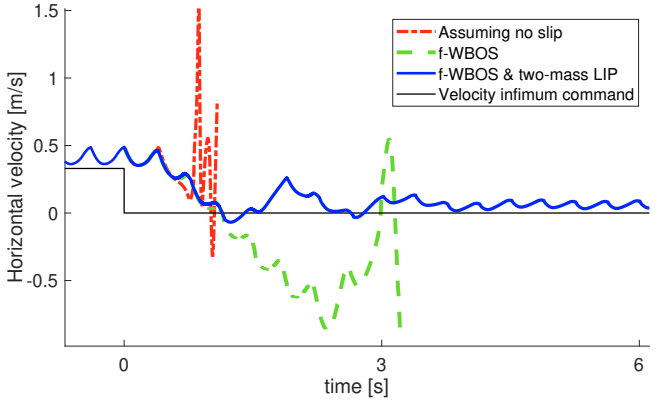

Fig. 6. Forward progression velocity during transition to the low-friction surface under three different controllers. Blue: the proposed control algorithm. Green: Without considering slip in step planner. Red: assuming stationary contact between robot and the ground.

5. CONCLUSIONS

This paper demonstrated a comprehensive multi-level controller with explicit consideration of foot slip for bipel robots. The reduced-order model was specifically selected such that it can describe the full-order model regardless of ground contact conditions. The reduced-order TMLIP model was then used for step planning, generating a set of reference trajectories to be followed by the whole-body controller. Depending on the ground contact conditions, the proposed controller used the WBOS or FWBOS models to obtain appropriate joint torques. We have shown that by using an appropriate task, convergence of the task controller was guaranteed. Simulation results demonstrated that integration of the full- and reduced-order models was dynamically justified. We have also shown that explicitly considering slip at all stages of the controller design enlarged the envelope of stability, since the newly proposed controller was able to maintain stability at lower friction coefficients, where neglecting and partial consideration of slip resulted in falling.

ACKNOWLEDGEMENTS

This work was supported in part by US National Science Foundation under award CMMI-1762556.

REFERENCES

Chen, K., Trkov, M., Yi, J., Zhang, Y., Liu, T., and Song, D. (2015). A robotic bipedal model for human walking with slips. In *Proc. IEEE Int. Conf. Robot. Autom.*, 6301–6306. Seattle, WA.

Chen, T. and Goodwine, B. (2021). Robust gait design for a compass gait biped on slippery surfaces. *Robot. Auton. Syst.*, 140, 103762.

Ferreira, J.P., Franco, G., Coimbra, P.A., and Crisóstomo, M. (2020). Human-like gait adaptation to slippery surfaces for the nao robot wearing instrumented shoes. *Intl. J. Humanoid Robot.*, 17(03), 2050007.

Kajita, S., Kanehiro, F., Kaneko, K., Yokoi, K., and Hirukawa, H. (2001). The 3d linear inverted pendulum mode: A simple modeling for a biped walking pattern generation. In *Proc. IEEE/RSJ Int. Conf. Intell. Robot. Syst.*, 239–246. Osaka, Japan.

Khadiv, M., Moosavian, S.A.A., Yousefi-Koma, A., Sadedel, M., and Mansouri, S. (2017). Optimal gait planning for humanoids with 3d structure walking on slippery surfaces. *Robotica*, 35(3), 569–587.

Khatib, O. (1987). A unified approach for motion and force control of robot manipulators: The operational space formulation. *IEEE J. Robot. Automat.*, 3(1), 43–53.

Luo, J., Su, Y., Ruan, L., Zhao, Y., Kim, D., Sentis, L., and Fu, C. (2019). Robust bipedal locomotion based on a hierarchical control structure. *Robotica*, 37(10), 1750–1767.

Luo, J., Zhao, Y., Kim, D., Khatib, O., and Sentis, L. (2017). Locomotion control of three dimensional passive-foot biped robot based on whole body operational space framework. In *Proc. IEEE Int. Conf. Robot. Biomimet.*, 1577–1582. IEEE.

Ma, W.L., Or, Y., and Ames, A.D. (2019). Dynamic walking on slippery surfaces: Demonstrating stable bipedal gaits with planned ground slippage. In *Proc. IEEE Int. Conf. Robot. Autom.*, 3705–3711. Montreal, Canada.

Mihalec, M., Trkov, M., and Yi, J. (2021). Recoverability-based optimal control for a bipedal walking model with foot slip. In *Proc. Amer. Control Conf.*, 1766–1771. New Orleans, LA.

Mihalec, M., Trkov, M., and Yi, J. (2022). Balance Recoverability and Control of Bipedal Walkers with Foot Slip. *ASME J. Biomech. Eng.*, 144(5). article 051012.

Mihalec, M. and Yi, J. (2021). Control of a bipedal walker under foot slipping condition using whole-body operational space framework. In *Proc. IFAC Model. Estim. Control Conf.* Austin, TX.

Mihalec, M., Zhao, Y., and Yi, J. (2020). Recoverability estimation and control for an inverted pendulum walker model under foot slip. In *Proc. IEEE/ASME Int. Conf. Adv. Intelli. Mechatronics*, 771–776. Boston, MA.

Reher, J. and Ames, A.D. (2021). Dynamic walking: Toward agile and efficient bipedal robots. *Ann. Rev. Contr. Robot. Auton. Syst.*, 4, 535–572.

Trkov, M., Chen, K., and Yi, J. (2019). Bipedal model and hybrid zero dynamics of human walking with foot slip. *ASME J. Comput. Nonlinear Dyn.*, 14(10). 101002.

Trkov, M., Chen, K., Yi, J., and Liu, T. (2020). Inertial sensor-based slip detection in human walking. *IEEE Trans. Automat. Sci. Eng.*, 17(1), 348–360.

Winter, D.A. (2009). *Biomechanics and Motor Control of Human Movement*. John Wiley & Sons Inc., New York, NY, 4th edition.

Zhao, Y., Fernandez, B.R., and Sentis, L. (2017). Robust optimal planning and control of non-periodic bipedal locomotion with a centroidal momentum model. *Int. J. Robot. Res.*, 36(11), 1211–1242.